Modeling sand fabric evolution during cyclic loading

Modelisation de l' évolution de la structure du sable au cours des charges cycliques

A. G. PAPADIMITRIOU, Dr. Civil Engineer, National Technical University of Athens, Greece
G. D. BOUCKOVALAS, Associate Professor, National Technical University of Athens, Greece

ABSTRACT: Sand fabric evolution during loading has been related in the literature to various aspects of cyclic response, such as the rates of plastic strain and excess pore pressure accumulation, as well as the enhanced contraction upon load reversal following previous dilative response. This paper proposes a simple way to account for these effects of fabric evolution, by means of a fabric tensor, whose rate of evolution has been related to the rate of plastic volumetric strain. This tensor provides for a fabric evolution index, which multiplies the plastic modulus of two surface plasticity model. As formulated, this index can be incorporated into many existing constitutive models. Comparison of simulations, with and without this index, to actual tests illustrates its contribution to realistic modeling of sand response.

RÉSUMÉ: Dans la litterature, un rapport a été etabli entre l' évolution de la structure du sable et multiples aspets du comportement cyclique, comme le rhythme d' accumulation des déformations plastiques et des pressions interstitielles, et comme le retrecissement augmenté qui est observé à l' inversement du chargement après une phase dilatative. Pour simuler ces effets de l' évolution de la structure d' une façon simple, cet article propose un tenseur de structure, qui developpe en fonction de l' incrément de la déformation plastique volumetrique. Ce tenseur est utilisé pour obtenir les valeurs d' un indice de l' évolution de la structure, qui multiplie le module plastique d' un modèle de plasticité à deux surfaces. Cet indice est formulé d' une façon permettante son introduction dans plusieurs modèles constitutifs existants. Une comparaison des résultats expérimentaux aux simulations obtenues, sans et avec cet indice, illustre son importance pour la simulation réaliste du comportement du sable.

1 INTRODUCTION

The term sand 'fabric' in this paper denotes the orientation of particle contact planes and not of the particles themselves. This distinction is necessary given that, while particle contacts reorient themselves during shearing, this does not hold for the particles themselves (e.g. Oda et al. 1985). Among the various fabric indices that have been proposed in related literature (e.g. the inter-particle orientation diagrams of Oda 1972), only fabric tensors have proven useful from a practical point of view. This is due to the fact that the microscopic issue of fabric is being addressed in a macroscopic approach.

The significance of initial and load-evolving fabric in designating sand behavior has been established by multiple laboratory studies in the literature (e.g. Arthur et al. 1981, Oda et al. 1985). Besides its significance, fabric is a basic constitutive ingredient merely in micromechanical models (e.g. Chang et al. 1992). In macromechanical analytical approaches, fabric is rarely incorporated and this because it leads to relatively complex constitutive equations.

More specifically, initial fabric is usually reproduced by introducing initial translations and distortions on model surfaces or by incorporating anisotropic moduli. While the latter is straightforward, the former procedure is usually performed by incorporating modified stress invariants. For example, Liang & Shaw (1991) propose a modified first invariant $J_1' = \boldsymbol{\sigma} : \mathbf{c}$, where $\boldsymbol{\sigma}$ is the effective stress tensor, $\mathbf{c}$ is a second order fabric tensor and symbol **:** denotes the trace of the product of the two tensors. Similarly, Nova & Sacchi (1982) propose a modified second invariant $J_2' = 1/2\ \mathbf{s}\ \mathbf{d}\ \mathbf{s}$, where $\mathbf{s}$ is the deviatoric stress tensor and $\mathbf{d}$ is a fourth order fabric tensor.

To incorporate fabric evolution during loading has proven even more complex in the literature. For example, Baker & Desai (1984) propose to use joint stress and plastic strain invariants for defining model surfaces, while Liang & Shaw (1991) and Pastor (1991) propose the modification of all three invariants by incorporating fabric tensors of the appropriate order.

Of interest to this paper is incorporating the effect of sand fabric evolution during loading in a simple manner, i.e. without any modifications to stress invariants. The main target is to achieve quantitative accuracy for cyclic shearing paths, where this effect dominates the response, as will be explained in the following paragraph. Observe that the term 'shearing', instead of 'loading', is used hereafter, given that the proposed formulation has been defined and calibrated for shearing paths, i.e. paths characterized by large variations in the deviatoric stress ratio tensor $\mathbf{r} = \mathbf{s} / p$, where p is the mean effective stress.

The effect of initial fabric is considered not so important in cyclic shearing, given that successive shear cycles tend to undermine it. Nevertheless, this effect can also be incorporated in a simplified manner through the proposed formulation.

2 EFFECT OF FABRIC EVOLUTION DURING SHEARING IN THE LABORATORY

It is well established that particle contact planes reorient themselves during monotonic shearing and their contact normals tend to become co-axial with the major principal stress direction (e.g. Oda et al. 1985). This holds true until peak strength at least. If shearing is reversed at its early stages (i.e. well beyond peak strength), unloading is generally stiff and leads to partly only reversed fabric changes (e.g. Chen et al. 1988). This leads to stiffer response during reloading in the original direction (e.g. Arthur et al. 1981). In general, successive shear cycles of relatively small amplitude lead to a continuously stiffening unloading - reloading response (e.g. Ladd et al. 1977). Given that the aforementioned observations have been performed under drained conditions, one could argue that this continuously stiffening response is due to partly reversed density changes. However, this is not the case, since it has also been observed in undrained shearing, at least far from initial liquefaction (Seed & Booker 1977, Egglezos & Bouckovalas 1999).

When the successive shear cycles are of larger amplitude, mostly the unloading paths become significantly compliant (e.g. Ladd et al. 1977). In parallel, Ishihara et al. (1975) established that the unloading paths become compliant only when the shear reversal occurs beyond the Phase Transformation Line (PTL), i.e. only after dilation has occurred. The increased compliance upon shear reversal from beyond the PTL is what triggers an increase in the rates of excess pore pressure buildup and permanent strain accumulation near initial liquefaction and cyclic mobility conditions, respectively. Hence, the PTL can play the role of a threshold in stress space, which differentiates the stress-strain response. This is supported by studies of fabric evolution, which show significant changes during dilation (Nemat-Nasser & Tobita 1982), that can only lead to increased compliance upon shear reversal.

3 ANALYTICAL FORMULATION

For the purpose of an analytical description of fabric evolution, one must prescribe an elasto-plastic context as the womb. For this purpose, the recently developed plasticity model of Manzari & Dafalias (1997) is considered. Details on the model are beyond the scope of this paper. It is merely noted that the model aims at accurately predicting shearing paths (where **r** changes significantly), hence model surfaces are conical with apex at the origin of axes. The model succeeds in simulating cyclic shearing mainly via the kinematic hardening yield criterion and an appropriately defined non-associated flow rule. For the purpose of this paper, importance lies in the form of the yield surface and of the plastic strain rate $\mathbf{d\varepsilon^p}$. Specifically, the yield surface is a circular cone described by the following yield function:

$$f = [(\mathbf{s}-p\boldsymbol{\alpha}):(\mathbf{s}-p\boldsymbol{\alpha})]^{1/2}-(2/3)^{1/2}mp = 0 \tag{1}$$

where $p\boldsymbol{\alpha}$ denotes the location of the axis of the cone and $(2/3)^{1/2}mp$ corresponds to the cone opening. The loading direction **L**, i.e. the gradient of the yield function with respect to the effective stress tensor $\boldsymbol{\sigma}$, is given by:

$$\mathbf{L} = \mathbf{n} + (V/3)\mathbf{I} \tag{2}$$

where **I** is the second order identity tensor, V is scalar and **n** is the direction of **L** in the deviatoric stress plane. Note that $\mathbf{n} : \mathbf{n} = 1$. The plastic strain rate $\mathbf{d\varepsilon^p}$ is given by:

$$\mathbf{d\varepsilon^p} = \langle \Lambda \rangle [\mathbf{n} + (D/3)\mathbf{I}] \tag{3}$$

where $\langle\ \rangle$ are the Macauley brackets, which yield $\langle x \rangle = x$ for $x > 0$ and $\langle x \rangle = 0$ for $x \le 0$. Parameter D is scalar and takes positive values when a plastic state is under the PTL, while the opposite occurs beyond the PTL. In this way, the plastic volumetric strain rate $d\varepsilon_{vol}^p$ inherits the sign of D, since $d\varepsilon_{vol}^p = \text{trace}(\mathbf{d\varepsilon^p}) = \langle\Lambda\rangle D$. Parameter Λ is the scalar loading index given by:

$$\Lambda = 1/K_p\ \mathbf{L} : \mathbf{d\sigma} \tag{4}$$

where $\mathbf{d\sigma}$ is the effective stress rate and K_p is the plastic modulus of the formulation. In general, the plastic modulus K_p can be formulated as follows:

$$K_p = p\ h_b\ h_f \tag{5}$$

where h_b is a dimensionless decaying function of "distance" from the failure surface (bounding surface in Manzari & Dafalias 1997). Scalar h_f is a dimensionless index that incorporates the effect of fabric evolution during shearing in constitutive equations and whose form will be presented below.

Specifically, in the definition of scalar index h_f the use of a macroscopic second order fabric tensor **F** is employed as:

$$h_f = \frac{1 + \langle \mathbf{F} : \mathbf{I} \rangle^2}{1 + \langle \mathbf{F} : \mathbf{n} \rangle} \tag{6}$$

If this fabric tensor **F** is deconvoluted according to:

$$\mathbf{F} = \mathbf{f} + (f_{vol}/3)\mathbf{I} \tag{7}$$

where $f_{vol} = \text{trace}(\mathbf{F})$, then Equation 6 can be rewritten in terms of **f** and f_{vol} according to:

$$h_f = \frac{1 + \langle f_{vol} \rangle^2}{1 + \langle \mathbf{f} : \mathbf{n} \rangle} \tag{8}$$

Based on Equation 8, when f_{vol} increases then the value of h_f increases as well and leads to a smaller plastic strain rate, according to Equations 3, 4 & 5. On the contrary, when $\mathbf{f} : \mathbf{n}$ increases then the opposite is observed. In all cases, scalar h_f takes merely positive values, due to the included Macauley brackets.

Complete definition of the fabric evolution function h_f requires a specific form for the evolution of fabric tensor **F**. Based on the above, the role of **F** can be deconvoluted into the roles of f_{vol} and **f**, which are distinctly different. Similarly, the definition of rates df_{vol} and **df** are also given a distinctly different form. Their common ground is the correlation of fabric evolution to dilative or contractive behavior, which was described in paragraph 2. Specifically, both rates are related to the plastic volumetric strain rate $d\varepsilon_{vol}^p$, which effectively distinguishes between dilative or contractive behavior based on its sign.

In general form, these rates are given by:

$$df_{vol} = A\ d\varepsilon_{vol}^p \tag{9a}$$

$$\mathbf{df} = -B \langle -d\varepsilon_{vol}^p \rangle [C\mathbf{n} + \mathbf{f}] \tag{9b}$$

where A, B and C are model parameters. According to Equation 9a, f_{vol} develops during all paths characterized by $d\varepsilon_{vol}^p \neq 0$, i.e. f_{vol} follows practically the whole shear history of the sand. This is not the case for **f**, which develops only when $d\varepsilon_{vol}^p < 0$ due to the Macauley brackets included in Equation 9b. In other words, **f** develops only during dilation and in the opposite sense to tensor $C\mathbf{n} + \mathbf{f}$. Observe that, while parameters A and B control the rate of f_{vol} and **f** development, parameter C corresponds to the max norm of **f**. This because, with **f** developing as above, $\mathbf{f} = -C\mathbf{n}$ will eventually be reached where $\mathbf{df} = \mathbf{0}$ until a potential shear reversal, which would change the direction of **n**.

To clarify the operation of Equation 9 and thus of the fabric evolution index h_f in Equation 8, Figure 1b presents a simulation of the undrained triaxial path in Figure 1a. Note that the test data presented in Figure 1a originate from Ishihara et al. (1975). Obviously, the numerator of h_f changes constantly during shearing that produces plastic strains. Hence, all along a shear path that remains under the PTL (where $d\varepsilon_{vol}^p > 0$, e.g. path 1÷a), f_{vol} and thus the numerator of h_f increases. This trend is reversed during shearing beyond the PTL (where $d\varepsilon_{vol}^p < 0$, e.g. paths a÷6, b÷8). Nevertheless, the numerator never takes values less than 1, because of the included Macauley brackets.

Unlike the numerator, the denominator of h_f does not follow the whole shear history. For example, all along shear path 1÷a, that remains under the PTL (where $d\varepsilon_{vol}^p > 0$), tensor $\mathbf{f} = \mathbf{0}$ and the denominator remains equal to 1. When the shear path continues beyond the PTL (e.g. path a÷6), tensor **f** begins to develop. Nevertheless, the value of the denominator remains equal to 1 during this dilative shear path, because **f** develops in the opposite sense of **n** and thus $\langle \mathbf{f} : \mathbf{n} \rangle = 0$. The denominator becomes larger than 1, only after a shear reversal that follows a dilative path (e.g. at point 6, following path a÷6). The value it takes is constant and corresponds to the value of **f** developed during the preceding path a÷6. This value is maintained until the next shear reversal (e.g. at point 7) or until tensor **f** starts developing in the opposite sense (i.e. beyond the PTL in extension).

Although parameters A, B and C could be assumed independent for greater simulative accuracy, for practical applications it was found necessary to interrelate them according to:

$$C = \max|f_{vol}|^2 \tag{10a}$$

$$B = A \tag{10b}$$

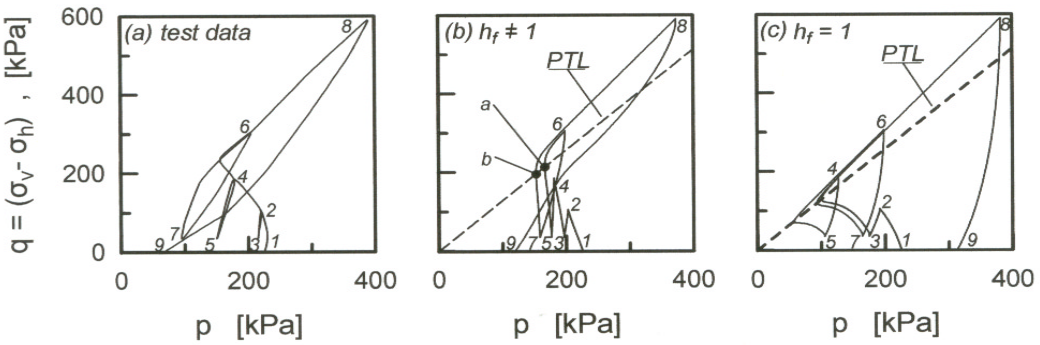

Figure1. Comparison of test data to simulations of an undrained triaxial path including shear reversals: a) test data (from Ishihara et al. 1975), b) simulation, which accounts for fabric evolution ($h_f \neq 1$), c) simulation, which ignores fabric evolution ($h_f = 1$).

In this way, the maximum value of the denominator becomes equal to $1+\max|f_{vol}|^2$, i.e. the maximum value ever retained by the numerator. Furthermore, Equation 10 establishes that the rate of change of the numerator with respect to $d\varepsilon_{vol}^p$ is more or less similar to the rate of change of the denominator with respect to $<- d\varepsilon_{vol}^p>$. Even more importantly from a practical point of view, in this way, the introduced fabric evolution index h_f necessitates only one additional parameter.

Finally, even an effect of initial fabric can be incorporated with the proposed formulation. It suffices that the value of **F** at consolidation is not set to zero, but is given an appropriate initial state value. For example, in the case of cross anisotropy its initial value could be characterized by $F_1 > F_2 = F_3$, where F_1, F_2 and F_3 are principal values.

4 SIMULATIONS OF EFFECT OF FABRIC EVOLUTION

Clearly, the importance of including h_f in model operation is not straightforward. For this purpose, Figure 1c presents another simulation of the shearing sequence of Figure 1a, for which the effect of fabric evolution during shearing is neglected, i.e. $h_f = 1$ (or A=0). By comparing the two simulations in Figures 1b & 1c it is deduced that only when $h_f \neq 1$ the constitutive model is able to simulate the continuously stiffening response for paths under the PTL (path 1÷a) that has been observed in the laboratory (see paragraph 2). This is a result of the evolving numerator of h_f, since the denominator remains equal to 1. In such cases, the introduced fabric tensor **F** practically "expands" in the sense that merely its first invariant f_{vol} increases, while its deviatoric component **f** remains equal to **0**. In this perspective, the role of the introduced formulation for cyclic shearing of small amplitude is partly an equivalent of an isotropically hardening cap.

As shown in Figure 1b, this hardening trend is reversed only upon unloading from points beyond the PTL, similarly to laboratory observations (see Figure 1a & paragraph 2). Furthermore, the "longer" the path beyond the PTL the more compliant is the simulated unloading (compare paths 6-7 and 8-9 in Figures 1a & 1b). By comparing the two simulations in Figures 1b & 1c it is deduced, that only when $h_f \neq 1$ the constitutive model can simulate these aspects of response upon unloading, which lead to higher excess pore pressures and a rapid decrease of effective stresses. Such simulations are mainly a result of the evolving denominator of h_f, where the introduced fabric tensor **F** is characterized by large variations in its deviatoric component **f**, which "redirect" the fabric tensor appropriately.

Furthermore, Figure 2 presents a similar comparison of two simulations to test data from a typical undrained triaxial test, where the shearing extends to both the compression and the extension side (2-way shearing). Note that Figures 2a, 2c & 2e compare the pertinent effective stress paths, while Figures 2b, 2d & 2f compare their respective stress-strain relations. Furthermore, note that the data of the triaxial test presented in Figures 2a & 2b originate from Arulmoli et al. (1992). To obtain a fair comparison, the plastic modulus K_p in the simulation of Figures 2e & 2f (where h_f=1, or A=0) was scaled up in order to attain the same excess pore pressure Δu after the first shear cycle in both simulations. Note how accounting for fabric evolution leads to the initially decreasing and eventually increasing rate of excess pore pressure build up that characterizes sand response (see Figure 2a, Seed & Booker 1977, Egglezos & Bouckovalas 1999). Furthermore, observe that only by incorporating fabric evolution the model simulates the characteristic compliant unloading paths that lead to values of p near zero (initial liquefaction).

The same comparison in terms of the stress-strain relation is performed in Figures 2b, 2d & 2f. Similar observations can be drawn, which underline the importance of accounting for fabric evolution for realistic simulations. For example, the simulation with $h_f = 1$ underestimates the effect of shearing the soil in extension and thus leads to rapid axial strain accumulation, which is not commonly observed in 2-way shearing tests in the laboratory (for example see Figure 2b).

Note that all simulations with $h_f \neq 1$ were performed with a fixed value of A = 8500. Furthermore, it is worth mentioning that the form of h_f presented herein is practically a generalization of a similar, but more simplified, fabric evolution index that was presented by Papadimitriou et al. (1999). In that case, the emphasis was on triaxial shearing alone and a simplified non-directional fabric evolution index h_f was used with success. In this case, which focuses on generalized shearing directions, the directivity of fabric evolution is considered mandatory and is thus incorporated through the use of fabric tensor **F**. For completeness it is noted, that Dafalias & Manzari (1999) proposed a deviatoric (i.e. f_{vol}=0) fabric tensor **f** effect on merely the flow rule of Manzari & Dafalias (1997). Their approach focused merely on accounting for enhanced contractive behavior upon shear reversal from above the PTL. The approach in this paper accounts for the whole shear history of the sand, from consolidation up to initial liquefaction or cyclic mobility.

5 CONCLUSIONS

The second-order tensor **F** introduced herein is a macroscopic constitutive element, which, in conjunction with the introduced fabric evolution index h_f that multiplies the plastic modulus K_p of the formulation, has been shown to provide increased accuracy in simulations of the cyclic shearing of sand. It plays the role of both an isotropically hardening cap for relatively small amplitude shear cycles, but also accounts for the enhanced contractive trend of sand upon shear reversals following dilative paths.

This tensor should not be considered as a direct representation of particle contact orientation.

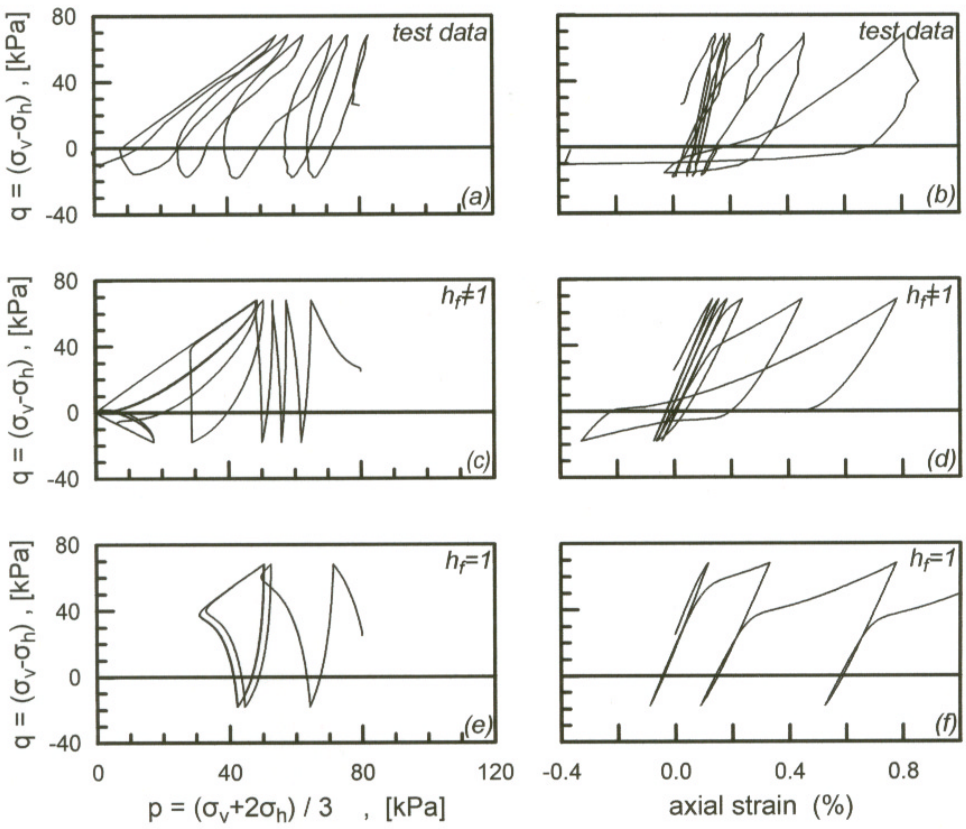

Figure 2. Comparison of test data to simulations of an undrained cyclic triaxial test: a & b) test data (from Arulmoli et al. 1992), c & d) simulation, which accounts for fabric evolution ($h_f \neq 1$) , e & f) simulation, which ignores fabric evolution ($h_f = 1$).

Nevertheless, its use via h_f is practically an indirect representation of the effect of fabric evolution on the measured response.

Finally, observe that a large number of constitutive models can be reformulated similarly to Equations 2 through 5. Hence, the introduction of a scalar fabric index h_f in the plastic modulus K_p of a formulation presented herein is not model-specific, but can be incorporated to many existing constitutive formulations.

6 ACKNOWLEDGEMENTS

The authors acknowledge financial support from the "Archimedes" basic research fund of the Institute of Communication & Computer Systems (ΕΠΙΣΕΥ) of the National Technical University of Athens.

7 REFERENCES

Arthur J. R. F., Bekenstein S., Germaine J. T. & C. C. Ladd 1981. Stress path tests with controlled rotation of principal stress directions. Laboratory Shear Strength of Soil ASTM, STP 740.

Arulmoli K., Muraleetharan K., Hossain M. & L. S. Fruth 1992. VELACS: VErification of Liquefaction Analyses by Centrifuge Studies; Laboratory Testing Program - Soil Data Report. *Research Report*, The Earth Technology Corporation.

Baker, R. & Desai C. S. 1984. Induced anisotropy during plastic straining. *International Journal of Numerical & Analytical Methods in Geomechanics*, 8: 167-185.

Chang C. S., Chang Y. & M. G. Kabir 1992. Micromechanics modelling for stress strain of granular soils. I: Theory. *Journal of Geotechnical Engineering ASCE* 118(12): 1959-1974.

Chen Y.-C., Ishibashi I. & G. T. Jenkins 1988. Dynamic shear modulus and fabric: part I, depositional and induced anisotropy. *Geotechnique* 38(1): 25-32.

Dafalias, Y. F. & Manzari M. T. 1999. Modeling of fabric effect on the cyclic loading response of granular soils. *Proceedings, 13th ASCE Engineering Mechanics Conference*, Baltimore (in CD-ROM).

Egglezos D. N. & G. B. Bouckovalas 1999. Permanent strain and pore pressure relations for cyclic loading of sand. *Proceedings, 2nd International Conference on Earthquake Geotechnical Engineering*, Lisbon, 1: 131-136, Rotterdam: Balkema.

Ishihara K., Tatsuoka F., & S. Yasuda 1975. Undrained deformation and liquefaction of sand under cyclic stresses. *Soils and Foundations* 15(1): 29-44.

Ladd C. C., Foott K., Ishihara F., Schlosser F. & H. G. Poulos 1977. Stress-deformation and strength characteristics. *State-of-the-art report. Proceedings, 9th International Conference on Soil Mechanics and Foundation Engineering*, Tokyo, 2: 421-494.

Manzari M. T. & Dafalias Y. F. 1997. A critical state two-surface model for sands. *Geotechnique* 47(2): 255-272.

Nemat-Nasser S. & Y. Tobita 1982. Influence of fabric on liquefaction and densification potential of cohesionless sand. *Mechanics of Materials* 1: 43-62.

Nova R. & G. Sacchi 1982. A model of the stress-strain relationship of orthotropic geological media", *Journal of Mechan. Theor. Appl.* 1, 6: 927-949.

Oda M. 1972. Initial fabrics and their relations to mechanical properties of granular materials. *Soils and Foundations* 12(1): 17-36.

Oda M., Nemat-Nasser S. & J. Konishi 1985. Stress-induced anisotropy in granular materials. *Soils and Foundations* 25(3): 85-97.

Papadimitriou, A. G., Bouckovalas G. D. & Y. F. Dafalias 1999. Use of elastoplasticity to simulate cyclic sand behavior. *Proceedings, 2nd International Conference in Earthquake Geotechnical Engineering*, Lisbon, Rotterdam: Balkema.

Pastor, M. 1991. A generalized plasticity model for anisotropic behaviour of sand. In Beer, Booker & Carter (eds.), *Computer Methods and Advances in Geomechanics*. Rotterdam: Balkema.

Seed H. B. & J. R. Booker 1977. Stabilization of potentially liquefiable sand deposits. *Journal of the Geotechnical Engineering Division ASCE* 103(7): 757-768.